JOM, Vol. 67, No. 4, 2015
DOI: 10.1007/s11837-015-1324-9

Nanomechanical Characterization and Protein Adsorption of Cold-Rolled Zirconium Alloy

PRAMANSHU TRIVEDI,[1] ANUP KUMAR PATEL,[1] RITA MAURYA,[1] R. JAYAGANTHAN,[2] and KANTESH BALANI[1,3]

1.—Biomaterials Processing and Characterization Laboratory, Department of Materials Science and Engineering, Indian Institute of Technology Kanpur, Kanpur 208016, India. 2.—Department of Metallurgical and Materials Engineering, Indian Institute of Technology Roorkee, Roorkee 247667, India. 3.—e-mail: kbalani@iitk.ac.in

The success of the implants used for bone regeneration and repair is highly dependent on the cell material interaction, which is further influenced by interaction of body proteins with the implant materials. In this study, a novel nanostructured Zircaloy-2 has been developed using cold rolling (reduction of 25%, 50%. 75%, and 85%), which resulted in the refinement of grains by several orders of magnitude. Phase analysis was done using x-ray diffraction, and the microstructures of room-temperature rolled Zircaloy-2 were obtained using optical microscopy. The adsorption behavior of bovine serum albumin as a function of protein concentration on Zircaloy-2 was performed, and the wettability before and after protein adsorption on Zircaloy-2 samples was estimated by measuring the contact angle of a water droplet on the processed samples. Nanoindentation studies were performed, which indicated higher hardness (of 2.15 GPa) and reduced elastic modulus (47.4 GPa) when compared with that of as-received Zircaloy-2 (hardness of ~0.12 GPa and reduced elastic modulus of 5.6 GPa). Also, it was found that protein adsorption increases to 0.59 mg/cm^2 for maximum deformed samples when compared with that of 0.38 mg/cm^2 for as-received samples. Contact angle decreased with increasing reduction from 62° (of the as-received sample) to 44° (at a reduction of 85%). But after protein adsorption, a further decrease in the contact angle from 43° (as received) to 26° (for 85% reduction) was observed. Thus, the engineered cold rolling can allow tailoring the nanomechanical properties of Zircaloy-2 while rendering the required protein adsorption as potential implant material.

INTRODUCTION

The biomaterials used for orthopedic application should not only exhibit desired bulk mechanical properties for the replacement of damaged tissue, but also they should possess supporting biological properties toward achieving rapid wound healing. Bone injuries and their failure require a deep inspection of biomaterials. Thus, research in this area is receiving extensive attention.[1,2] Several classes of bone materials such as polymers, metals, and ceramics have been explored to replace these damaged and diseased bones.[3–5] For the success of these implant materials, an understanding of cell material interaction can provide an insight into their applicability for intended functionality. The interaction of cell materials plays a crucial role in influencing the processes of cell adhesion, cell proliferation, and differentiation on the implant surface.[6–9] Cells do not contact the implant surface directly; rather, the implant material first comes in contact with the proteins present in the body fluid followed by attachment of the cells with these proteins. Hence, the study of protein adsorption behavior is an important factor in determining the ultimate biocompatibility of the implant material.

Metallic implants such as Co-Cr-Mo type alloys, stainless steel (316L), Ti and its alloys (Ti-6Al-4V), Zr alloys (Zr-2.5Nb) are some of the widely used materials in orthopedics and dental implants.

(Published online February 12, 2015)

Among these, Zr and its alloys have attained extensive focus due to their superior mechanical properties and excellent biocompatibility, which makes these alloys attractive for using as surgical implants.[10–14] Zircaloy-2 emerges as favorable implant material due to improved corrosion resistance, specially pitting susceptibility, and enhanced biocompatibility compared with that of other zirconium alloys such as Zr-2.5Nb.[15] *In vivo* studies on Zr alloys have indicated that Zr and its alloys show good osteointegration,[16,17] and when compared with Ti alloys, they possess a higher degree of bone implant contact.[18,19] *In vitro* studies on zirconium and its alloys have been carried out by a number of researchers.[15,20] The oxide layer (ZrO_2) formed on the surface of Zr and its alloys is known to be chemically stable in various environments along with good mechanical strength and excellent wear and corrosion resistance. The biocompatibility and wear properties of ZrO_2 layer makes it one of the most suitable materials to be used as ceramic ball head in total hip replacement devices.[21]

In the past few years, the development of ultrafine grained materials has gained increased interest due to their superior mechanical properties when compared with that of conventional alloys. The metals processed through severe plastic deformation, such as accumulative roll bonding, equal-channel angular pressing, severe rolling, and multiaxial forging, find applications as bulk structural components.[22–24] The literature available on the effects of nanostructured surfaces on the biological properties is well known: Webster and Ejiofor[25] reported enhanced osteoblast adhesion on nanophase Ti6Al4V alloy. Saldan et al.[26] reported the biocompatibility of ultrafine-grained Zr alloy rolled up to 75% thickness reduction, followed by annealing at 700°C. But the grain size effect has not shown any significant effect on biocompatibility due to grain growth during annealing. In a recent study conducted by Mordyuk et al.,[27] ultrafine grains of about 20 μm size were reported in Zr-1%Nb cold-rolled alloy (up to 75% thickness reductions), but their effect on biocompatibility has not been reported.

In a previous work, the biocompatibility of cryorolled Zircaloy-2 was investigated,[15] and the tensile strength of cryorolled Zircaloy-2 was shown to increase to 726 MPa compared with that of as-received Zircaloy-2 (from 592 MPa). Grain size reduction from 10 μm to 183 nm occurred (after cryorolling at liquid nitrogen), resulting in an increased biocompatibility and differentiation of the cells. Detailed bulk mechanical and structural properties of room-temperature (RT) rolled Zircaloy-2 have already been reported.[28] But, the nanomechanical properties and the effect of protein adsorption and wettability correlation on cold-rolled Zircaloy-2 have not been reported in the literature.

In the current work, the nanomechanical behavior of severely rolled Zircaloy-2 (up to 85% reduction and other samples reported in processing of Zircaloy-2 by cold rolling) has been investigated. The study also deals with the adsorption behavior of bovine serum albumin (BSA) protein on the rolled samples after 24 h of incubation in humidified atmosphere and dependence of wettability on the samples before and after protein adsorption.

MATERIALS AND METHOD

Cold Rolling of Zircaloy-2

The Zircaloy-2 used in this study was procured from NFC (Hyderabad, India) as 4.5-mm-thick rolled sheets.[15] The chemical composition of Zircaloy-2 is 1.3–1.6% Sn, 0.07–0.20% Fe, 005–0.16% Cr, 0.03–0.08% Ni, 0.006% N, and rest Zr. The as-received material (named as ASR) was heated in the Ar atmosphere at 800°C followed by quenching in mercury at room temperature (named the HgQ sample). Then, room-temperature rolling was carried out on HgQ samples to achieve different reductions, i.e., 25% (RT-25), 50% (RT-50), 75% (RT-75), and 85% (RT-85). These samples were compared with ASR and HgQ samples as control/reference material. In order to achieve same roughness level on samples, the rolled material was ground sequentially on emery papers of grit size 800–1600, followed by cloth polishing using 1-μm size alumina slurry. The rolling was performed at 0.2–0.05 mm thickness reduction per pass using two high-rolling mills (110 mm roll diameter) at 8 rpm. After every pass, the samples were dipped into water to avoid heating, if any. During rolling, $MoSiO_2$ lubricant was used to reduce friction losses and heat.

Phase and Microstructural Characterization

The phases of rolled Zircaloy-2 were characterized by x-ray diffraction (2000D diffractometer; Rich-Seifert) using Cu-Kα having a wavelength of 1.54 Å at the scan rate of 1° per minute (step size of 0.02°). The microstructures of Zircaloy-2 samples were obtained by using optical microscopy (DeWinter), and the grain size was quantified using ImageJ software (version 1.0).

Protein Adsorption

The protein adsorption behavior was quantified using standard protein adsorption protocol as given in bicinchoninic acid protein quantification assay kit. An equal amount of initial protein concentration of 2 mg/mL was filled into 24 well plates containing Zircaloy-2 samples. The well plate was then placed in an incubator for 24 h, which provided a temperature of 37°C, was humidified, and consisted of 5% CO_2/95% air. After an incubation period of 24 h, each sample was gently rinsed with PBS to remove non adhered proteins. Then the samples were washed with a RIPA (Sigma) buffer for 10 min. The protein concentration of every eluted sample was estimated as per standard bicinchoninic acid protocol instructions. This assay is based on the

reduction of Cu^{2+} to Cu^{1+} by protein in an alkaline medium through selective colorimetric detection of cuprous cation (Cu^{1+}) by bicinchoninic acid. The protein reacts with Cu^{2+}, resulting in a change from blue to violet color complex, which absorbs light at 540 nm. The color change was quantified using ultraviolet-vis (Bio-Tek) at wavelengths between 540 nm and 570 nm. An average of three tests is reported in the current work. Statistical Student t test analysis was carried out to confirm the confidence level of more than 95% ($p < 0.05$).

Wettability

To correlate the effect of wettability on grain size and protein adsorption, the contact angles were measured (10 readings each on three samples) both before and after the protein adsorption. Wettability behaviors of Zircaloy-2 samples were analyzed by using a computer-controlled goniometer (Dataphysics Contact Angle System OCA) performing sessile drop contact angle measurement with distilled water droplets (volume of ~10 μL). The samples were polished to equal roughness scale of about 100 nm to minimize the roughness effect on the contact angle values. Then samples were ultrasonically cleaned in 70% vol/vol ethanol, followed by final rinsing with distilled water before air drying.

Nanoindentation

Nanoindentation is represented as load–displacement plots of indentations performed at 200 μN indentation-load (loading rate of 40 μN/s with a dwell time of 2 s at maximum load) on the samples rolled at different reduction percentages. An experimental analysis was carried out using load-time sequence as per Oliver and Pharr's method.[29] It is reported in the literature that a lower indentation depth results in higher hardness values, whereas a steeper slope of unloading curve results a higher reduced modulus (E_r).[29] Therefore, loading and unloading of the indenter was carried out four times in succession at a fixed loading rate/load ($1/P\ dP/dt$) to maintain a constant loading-rate/load ($1/P\ dP/dt$) [or constant indentation strain rate ($1/h\ dh/dt$)].[30]

Nanoindentation tests were carried out on ASR, HgQ, and room-temperature rolled samples using a Hysitron TI 750-D Ubi-1 model. The elastic modulus and hardness were estimated by using a continuous stiffness option, which results in elastic modulus and hardness as a function of indentation depth. Indentation was performed by using a Berkovich indenter, with a tip having a pyramidal shape possessing a phase angle of 65.35° and edge to opposite side angle of 142.35°, and tip radius of 150 nm. As the indentation width is quite large (a few micrometers), each indent is expected to fall across a few grains (because the biggest grain is ~11.5 μm and the lowest one is ~200 nm). An average value from 10 indentations is reported for the obtained hardness and reduced elastic modulus.

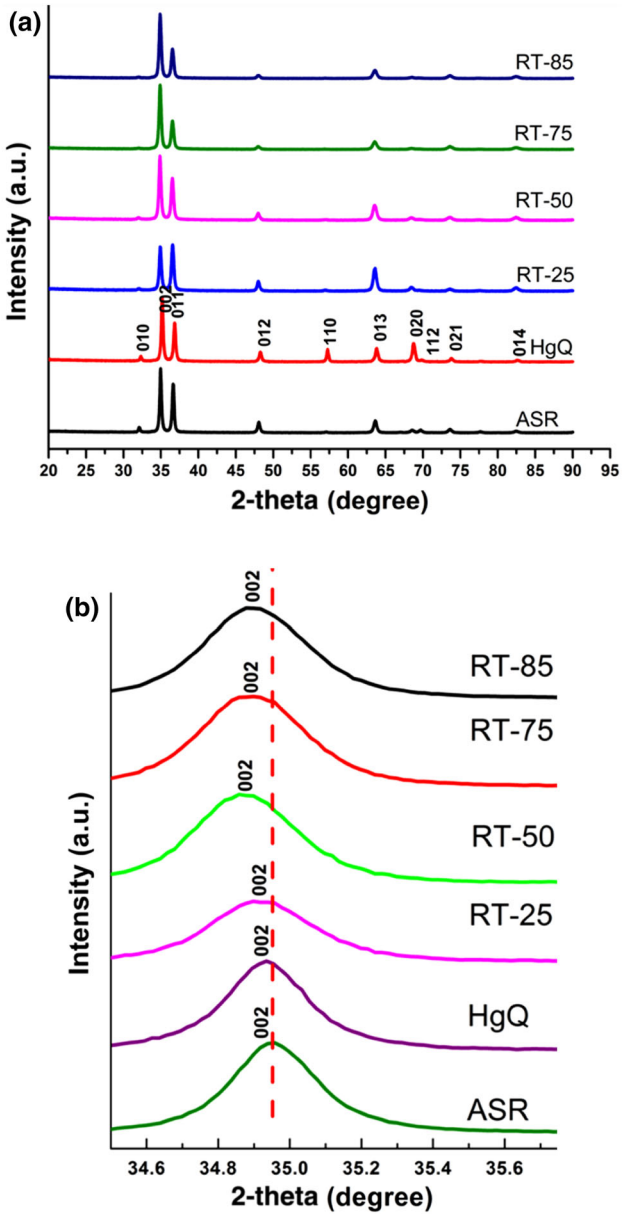

Fig. 1. X-ray diffraction patterns of (a) Zircaloy-2 samples. (b) Expanded view showing broadening and shifting of (002) peak after cold rolling.

RESULTS AND DISCUSSION

Phase and Microstructure Analysis

X-ray diffraction revealed the presence of α phase in the as-received Zircaloy-2, as shown in Fig. 1a. All the peaks shown in the pattern matched with reference pattern (98-007-1958) as reported for α phase of Zircaloy-2 in inorganic crystal sample data. It was reported in earlier work[15,28] that the room-temperature rolling progresses to different thickness reductions, i.e., 25%, 50%, 75%, 85% results an increase in the dislocation density from $1.61 \times 10^{15}/m^2$ for HgQ to $15.47 \times 10^{15}/m^2$ for 85% room-temperature rolled (RT-85) material. Figure 1b shows

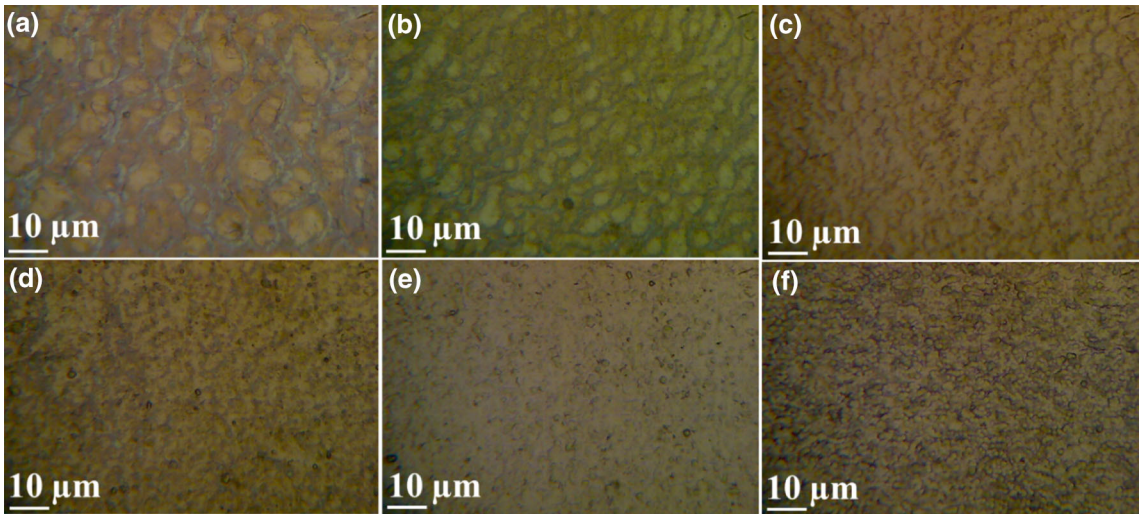

Fig. 2. Optical images of zircaloy-2 samples: (a) ASR, (b) HgQ, (c) RT-25, (d) RT-50, (e) RT-75, and (f) RT-85.

Table I. Average grain size and crystallite size of zircaloy-2 samples

Sample name	Reduction, %	Average grain size, μm	Crystallite size, nm
ASR	–	11.4 ± 4.2	142 ± 24
HgQ	–	8.1 ± 3.1	121 ± 18
RT-25	25	4.4 ± 2.2	87 ± 11
RT-50	50	1.2 ± 0.6	65 ± 14
RT-75	75	0.9 ± 0.3	34 ± 10
RT-85	85	0.6 ± 0.3	23 ± 11

broadening and shifting of peaks as the deformation takes place from HgQ to RT-85. Apart from limited crystallite size, the broadening is also contributed to the high dislocation densities present in the deformed samples. Shifting in the HgQ is toward the lower 2θ values (Fig. 1b), which arises due to the fact that HgQ samples were annealed at 800°C followed by quenching, indicates generation of residual compressive stresses. In the case of the cold-rolled samples, shifting toward lower 2θ values (Fig. 1b, compared to HgQ sample) is expected due to an increased reduction percentage, which results in a higher degree of internal stresses.

Regarding the microstructural analysis, Fig. 2 shows that the grain size decreases from 11.4 μm for ASR (Fig. 2a) and 8.1 μm for HgQ (Fig. 2b) to 0.6 μm as the reduction percentage increases in cold-rolled Zircaloy-2 samples (Fig. 2c–f; Table I).

Protein Adsorption

Wettability and protein adsorption on a biomaterial surface significantly affect the cell adhesion, cell proliferation, and cell differentiation.[31] Figure 3 shows the adsorbed protein density on Zircaloy-2 samples. It is evident from the figure that the adsorbed protein density increases from 0.38 mg/cm^2 for ASR to 0.59 mg/cm^2 for RT-85. Whereas for RT-25 and RT-50, the adsorbed protein density is 0.41 mg/cm^2 and 0.44 mg/cm^2, which is very close to that of ASR sample's adsorption. But for of RT-75, the protein adsorption density (of 0.52 mg/cm^2) is almost similar to that of RT-85. It has been reported in the literature that the nanotexture in materials favored cell adhesion when compared with that of conventional (coarse grained) material.[32] Thus, it could be expected from these results that cold-rolled Zircaloy-2 samples could also exhibit favored protein adsorption. The same is confirmed from Fig. 3, which confirms that as the grain size of the material decreases (with increase in reduction percentage from ASR to RT-85), the adsorbed protein density increases by more than 1.5 times. The results also corroborates well with the wetting behavior of the Zircaloy-2 samples as discussed later. It is seen that as the wetting behavior of the surface increases, the adsorbed protein concentration also increases. The reason for this behavior may be attributed to the hydrophilic functional groups present in bovine serum albumin protein.

Wettability

It is evident from the previous reports on correlation between protein adsorption and cell adhesion behavior that high concentration protein on the implant surface leads to higher cell density.[33] Hence, the correlation of wettability and protein

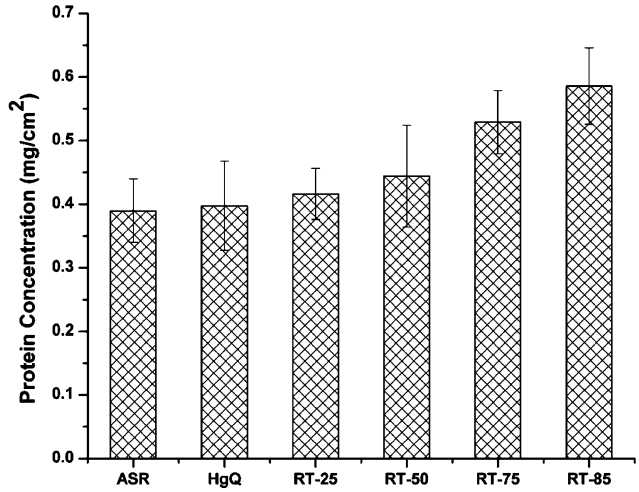

Fig. 3. Protein adsorption behavior on the surface of Zircaloy-2 samples.

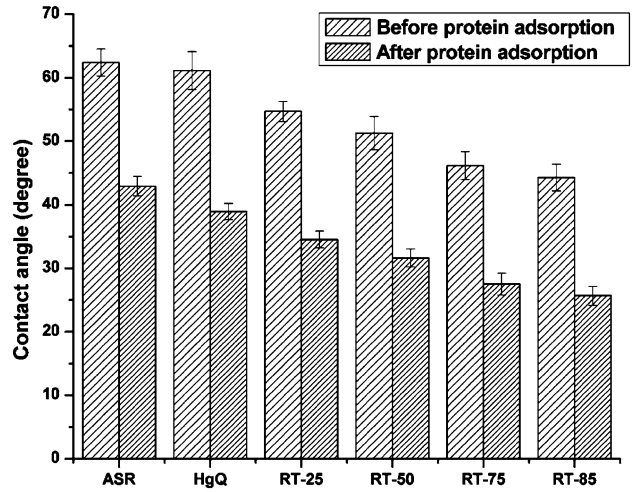

Fig. 4. Contact angle of water droplet on Zircaloy-2 samples surface.

adsorption is important for engineering the required functionality of the implant. Figure 4 shows the contact angle measurement on Zircaloy-2 surfaces before and after protein adsorption. It is evident from that contact angle that protein decreases from 62° for ASR to 44° for RT-85 (Fig. 4). After protein adsorption, there is a further decrease in the contact angle from 43° for ASR to 26° for RT-85 (Fig. 4). A decrease in the contact angle after adsorption of protein could be explained through the surface wettability.[34] As the grain size reduction occurs, an increase in surface-energy enhances the wettability of the surface. As the protein adsorption on the samples surface increases, a further decrease in the contact angle is observed, which can be attributed to the hydrophilic functional groups present in the protein.

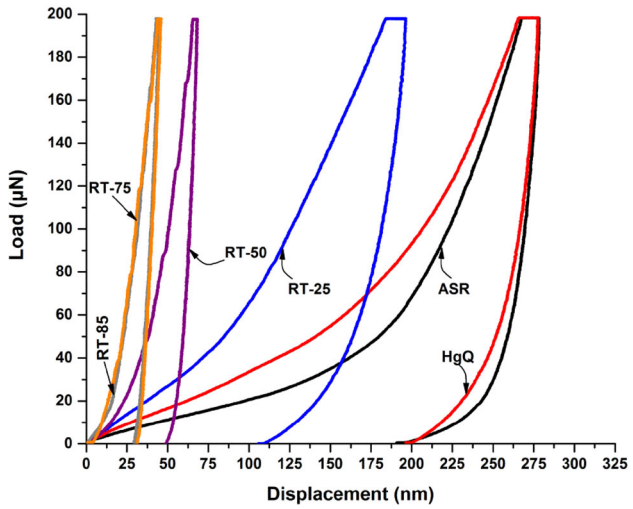

Fig. 5. Nanoindentation of Zircaloy-2 samples.

Nanoindentation

It is evident from Fig. 5 that as the reduction ratio increases, the indentation depth is observed to decrease (i.e., the slope of the unloading curve increases and slopes becomes steeper) in the similar fashion, indicating a higher hardness and higher stiffness of the rolled materials. It could be seen from Fig. 5 that RT-85 and RT-75 have the least indentation depth (~42 nm and 45 nm, respectively) when compared with that of ASR and HgQ samples (which showed indentation depths of 298 nm and 278 nm, respectively). The other samples, viz. RT-25 and RT-50, have also shown significantly lower indentation depths, i.e., 197 nm and 68 nm, respectively, when compared with that of the ASR sample. Table II shows reduced modulus and hardness of Zircaloy-2 samples. The reduced modulus increased to 47.6 GPa for the RT-85 sample, although for ASR samples, the reduced is a meager 5.6 GPa. Similarly, the hardness values have increased from 0.2 GPa for ASR to 2.26 GPa for RT-85. The reason for the increase in the hardness and reduced modulus values might be due to the fact that as the reduction ratio increases, grain size decreases resulting in the large number of grain boundaries, which hinder the indentation, resulting in an increased hardness and reduced modulus values. Furthermore, the internal stresses might also play a part in affecting the recovery (and thus material's stiffness) during unloading. The results of nanomechanical properties (such as hardness) corroborate well with the bulk properties reported in the literature.[28]

Figure 6 summarizes the effect of cold rolling (and grain size reduction) on the protein adsorption of Zircaloy-2. It is evident that cold-rolled Zircaloy-2 (to different thickness reductions of 25, 50, 75, and 85%), increase protein adsorption as the reduction percentage increases. It could be inferred that a higher reduction percentage enhances the surface

Table II. Hardness (H) and reduced modulus (E_r) of zircaloy-2 obtained by nanoindentation

Sample	E_r, GPa	H, GPa	H_f, nm	H_m, nm
ASR	5.6 ± 0.7	0.12 ± 0.08	298	197
HgQ	9.9 ± 1.1	0.13 ± 0.06	278	192
RT-25	23.5 ± 1.7	0.45 ± 0.03	197	107
RT-50	33.6 ± 1.1	0.95 ± 0.04	68	49
RT-75	45.5 ± 1.4	1.96 ± 0.05	45	29
RT-85	47.4 ± 1.2	2.15 ± 0.63	42	26

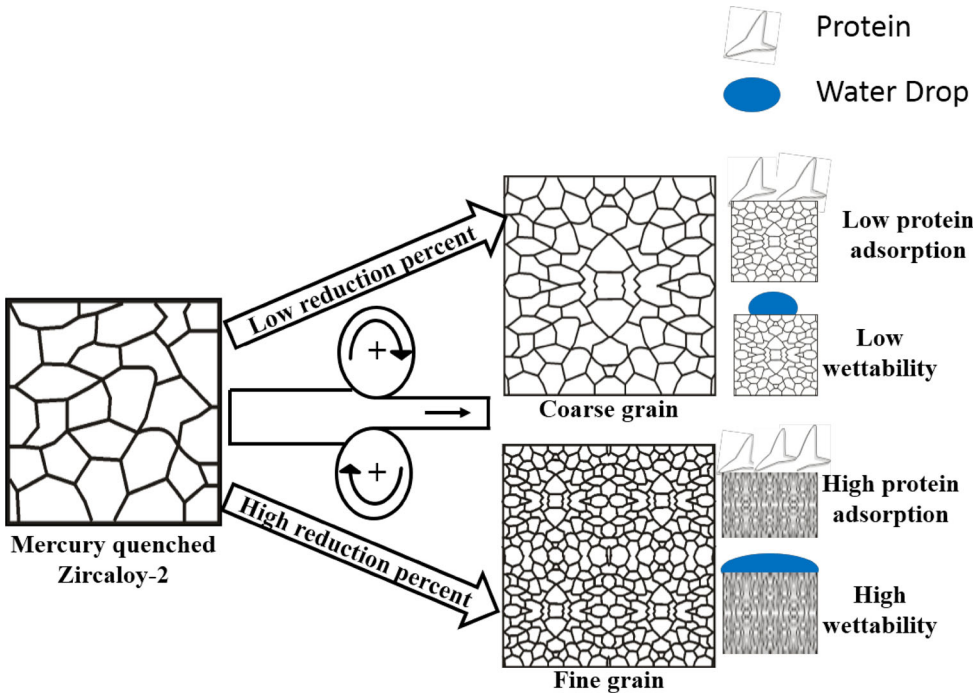

Fig. 6. Effect of grain size on protein adsorption and wettability.

energy, and in conjunction with increased internal stresses, surface relaxation is resulting in enhanced wettability. Furthermore, a reduction in the grain size has also shown a dramatic increase in the hardness (by ~17.9 times) and reduced elastic modulus (by ~8.5 times).

CONCLUSION

Cold rolling of Zircaloy-2 to various reduction percentages (as received, HgQ, and reduction percentages of 25, 50, 75, and 85) has elicited the correlation of grain refinement on their nanomechanical properties. Furthermore, the role of grain size (via cold-rolling reduction) on the protein adsorption (1.5 times increased protein adsorption on RT-85 when compared with that of the ASR sample) conveys a strong contribution of surface energy on affecting the wettability of surface. It is evident that the nanomechanical properties of severely deformed materials are quite altered due to the presence of enhanced dislocation density and a reduction in the grain size (~by 19 times), showing an increase in the hardness (by 17.9 times) and reduced modulus by 8.5 times in RT-85 when compared with that of ASR. Thus, tailoring the grain size of the Zircaloy-2 by the cold-rolling process significantly improves the protein adsorption, wettability, and mechanical properties, which will make cold-rolled Zircaloy-2 find an application as a potential implant material.

ACKNOWLEDGEMENTS

Authors acknowledge Advanced Centre for Materials Science, IIT Kanpur, towards the use of nanoindentation facility.

REFERENCES

1. S.F. Amato, *Regulatory Affairs for Biomaterials and Medical Devices,* ed. S. Amato and B. Ezzell (New York: Elsevier, 2015), pp. 27–46.
2. N. Scarborough and N. Mukherjee, *Regulatory Affairs for Biomaterials and Medical Devices,* ed. S. Amato and B. Ezzell (New York: Elsevier, 2015), pp. 11–26.
3. L.L. Hench, *J. Am. Ceram. Soc.* 74, 1485 (1991).

4. D.W. Hutmacher, *Biomaterials* 21, 2529 (2000).
5. M. Niinomi, *Biomaterials* 24, 2673 (2003).
6. Z. Schwartz and B.D. Boyan, *J. Cell. Biochem.* 56, 340 (1994).
7. J.L. Ong, C.W. Prince, G.N. Raikar, and L.C. Lucas, *Implant Dent.* 5, 83 (1996).
8. J.Y. Martin, Z. Schwartz, T.W. Hummert, D.M. Schraub, J. Simpson, J. Lankford Jr, D.D. Dean, D.L. Cochran, and B.D. Boyan, *J. Biomed. Mater. Res.* 29, 389 (1995).
9. R.K. Sinha, F. Morris, S.A. Shah, and R.S. Tuan, *Clin. Orthop. Relat. Res.* 305, 258 (1994).
10. P. Gehrke, G. Dhom, J. Brunner, D. Wolf, M. Degidi, and A. Piattelli, *Quintessence Int.* 37, 19 (2006).
11. K.M. Sherepo, A.B. Parfenov, and I.S. Zusmanovich, *Med. Tekh.* 5, 14 (1992).
12. M. Niinomi, *JOM* 4, 32 (1999).
13. P. Thompsen, C. Larsson, L.E. Ericson, L. Sennerby, J. Lausmaa, and B. Kasemo, *J. Mater. Sci. Mater. Med.* 8, 653 (1997).
14. K.M. Sherepo and I.A. Redko, *Med. Tekh.* 2, 22 (2004).
15. P. Trivedi, S. Goel, S. Das, R. Jayaganthan, D. Lahiri, and P. Roy, *Mater. Sci. Eng. C* 46, 309 (2015).
16. R.L. Cabrini, M.B. Guglielmotti, and J.C. Almagro, *Implant Dent.* 2, 264 (1993).
17. M.B. Guglielmotti, C. Guerrero, and R.L. Cabrini, *Acta Odontol. Latinoam.* 10, 11 (1997).
18. M.B. Guglielmotti, S. Renou, and R.L. Cabrini, *Int. J Oral Maxillofac. Impl.* 14, 565 (1999).
19. O.B. Kulakov, A.A. Doktorov, S.V. Diakova, I.I. Denisov-Nikolskii, and K.A. Grotz, *Morfologiia* 127, 52 (2005).
20. E. Eisenbarth, D. Velten, M. Muller, R. Thull, and J. Breme, *Biomaterials* 25, 5705 (2004).
21. C. Piconi and G. Maccauro, *Biomaterials* 20, 1 (1999).
22. R.Z. Valiev and T.G. Langdon, *Prog. Mater. Sci.* 51, 881 (2006).
23. R.Z. Valiev, R.K. Islamgaliev, and I.V. Alexandrov, *Prog. Mater. Sci.* 45, 103 (2000).
24. R.Z. Valiev, *Nat. Mater.* 3, 511 (2004).
25. T.J. Webster and J.U. Ejiofor, *Biomaterials* 25, 4731 (2004).
26. L. Saldan, A. Mendez-Vilas, L. Jiang, M. Multigner, J.L. Gonzalez-Carrasco, M.T. Perez-Prado, M.L. Gonzalez-Martın, L. Munuera, and N. Vilaboa, *Biomaterials* 28, 4343 (2007).
27. B.N. Mordyuk, O.P. Karasevskaya, G.I. Prokopenko, and N.I. Khripta, *Surf. Coat. Technol.* 210, 54 (2012).
28. S. Goel, R. Jayaganthan, I.V. Singh, D. Srivastav, G.K. Dey, and N. Saibaba, *Mater. Des.* 55, 612 (2014).
29. W.C. Oliver and G.M. Pharr, *J. Mater.* 7, 1564 (1992).
30. B.N. Lucas, W.C. Oliver, G.M. Pharr, and J.-L. Loubet, *Materials Research Society Symposium Proceedings*, vol. 436, ed. W.W. Gerberich, H. Gao, J-E. Sundgren, and S. Baker (Cambridge, U.K.: Cambridge University Press, 1996), p. 233.
31. L. Ponsonnet, K. Reybier, N. Jaffrezic, V. Comte, C. Lagneau, M. Lissac, and C. Martelet, *Mater. Sci. Eng. C* 23, 551 (2003).
32. P. Trivedi, P. Gupta, S. Srivastavab, R. Jayaganthan, R. Chandra, and P. Roy, *Appl. Surf. Sci.* 293, 143 (2014).
33. D.D. Deligianni, N. Katsala, S. Ladas, D. Sotiropoulou, J. Amedee, and Y.F. Missirlis, *Biomaterials* 22, 1241 (2001).
34. J.I. Rosales-Leal, M.A. Rodríguez-Valverde, G. Mazzaglia, P.J. Ramon-Torregrosa, L. Díaz-Rodriguez, O. Garcia-Martinez, M. Vallecillo-Capilla, C. Ruiz, and M.A. Cabrerizo-Vílchez, *Coll. Surf. A* 365, 222 (2010).